$$\langle G(\vec{r},\vec{r}')\rangle = \sum_k \sum_{LL'} Y_L(\hat{r})(P^k + P^k W P^k + P^k W P^k W P^k + \cdots)_{LL'} Y_{L'}(\hat{r}')$$

$$= \sum_{LL'k} Y_L(\hat{r})[P^k(1 - WP^k)^{-1}]_{LL'} Y_{L'}(\hat{r}')$$

$$\equiv \sum_{LL'} Y_L(\hat{r}) G_{LL'} Y_{L'}(\hat{r}'), \quad \text{(A7)}$$

where P^k has matrix elements defined in Eq. (4.5). The last step in Eq. (A7) serves to define the matrix G that appears in Eq. (4.6).

*Present address: Department of Physics, Case Western Reserve University, Cleveland, Ohio 44106.

[1]Paul Soven, Phys. Rev. **156,** 809 (1967).
[2]B. Velický, S. Kirkpatrick, and H. Ehrenreich, Phys. Rev. **175,** 747 (1968).
[3]Paul Soven, Phys. Rev. B 2, 4715 (1970).
[4]L. Schwardz, F. Brouers, A. V. Vedyayev, and H. Ehrenreich, Phys. Rev. B **4,** 3383 (1971).
[5]J. L. Beeby, Phys. Rev. 135, A130 (1964); Paul Soven, Phys. Rev. **151,** 539 (1966).
[6]A.-B. Chen, G. Weisz, and A. Sher, Phys. Rev. B **5,** 2897 (1972).
[7]Equations (2.2) and (2.4) correspond to Eqs. (2.7) and (2.22) of Ref. 2, respectively. Note that Eq. (2.4) holds for general localized potentials.
[8]A comparison of the CPA and other single-site approximations in terms of moments and other relevant alloy parameters is summarized by L. Schwartz and E. Sigga, Phys. Rev. B **5,** 283 (1972).
[9]Equation (4.30) of Ref. 2.
[10]A.-B. Chen, Bull. Am. Phys. Soc. **17,** 325 (1972).
[11]Equation (13) of Ref. 1, or Eq. (16) of Ref. 3.
[12]For the discusssion of the effect of the excluded terms of the multiple scattering series, see R. M. More, in *Electronic Density of States,* edited by L. H. Bennett, U. S. Natl. Bur. Std. Spec. Publ. No. 323 (U. S. GPO, Washington, D. C., 1972), p. 515.
[13]Y. Onodera and Y. Toyozawa, J. Phys. Soc. Jap. **24,** 341 (1968), especially Eq. (2.11A).
[14]For example, the simple interpolation formula of Lagrange can be used. See H. Margenau and G. M. Murphy, in *The Mathematics of Physics and Chemistry* (Van Nostrand, Princeton, N.J., 1961), Sec. 13.3. Note that Eq. (3.12) corresponds to a linear Lagrange formula.
[15]The CPA self-energy has a pole at $E = \epsilon$ for the case $x = 0.15$ and $\delta = 1.5$. The behavior of the self-energy as a function of E is very similar to that shown in Fig. 5(c) of Ref. 2.
[16](S.9) means Soven's Eq. (9) in Ref. 3. The same notation will be used throughout.
[17]The Y_L is the same as Y_{lj} in F. G. Ham and B. Segall, Phys. Rev. **124,** 1786 (1961).
[18]The structure factors in Eq. (4.5) are the ones that appeared in Ref. 17.
[19]This type of sum in Eq. (4.5) is an essential task in all the CPA procedures. It also appeared in the other CPA formalism for muffin-tin potentials; for example, B. L. Gyorffy, Phys. Rev. B **5,** 2382 (1972), Eq. (16).

PHYSICAL REVIEW B VOLUME 7, NUMBER 6 15 MARCH 1973

Interpolation-Scheme Calculation of Electron-Phonon Interaction in Noble and Transition Metals: Copper*

Shashikala G. Das
Argonne National Laboratory, Argonne, Illinois 60439
and University of Chicago, Chicago, Illinois 60637

(Received 14 July 1972)

A simple method for evaluating the electron-phonon interaction matrix elements, and hence the point-mass enhancement and the relaxation time of quasiparticles, is proposed for the transition metals. The method is based essentially on the Bloch model of the electron-phonon interactions and is similar to a pseudopotential formulation with modification to account for the presence of d electrons in the conduction bands and the resulting anisotropy of the above quantities. The results obtained by applying our theory to copper, based on the combined interpolation scheme with explicit inclusion of the screening effects based on Lindhard's formulation and of the contributions from transverse and longitudinal phonons and from umklapp processes, are in fair quantitative agreement with those obtained from a phenomenological interpretation of the experimental cyclotron-mass data of Lee and with the calculations of Nowak based on an empirical phase-shift formulation.

I. INTRODUCTION

Although the importance of the electron-phonon interaction has been well demonstrated in superconductivity,[1] very little work has been done to demonstrate explicitly the nature and anisotropy of the electron-phonon interaction in transition metals. This is primarily due to the great complexity that the presence of the d bands near the conduction bands in such metals leads to. In simple metals the conduction bands, consisting essentially of s bands, are separated from the well-

localized d or f bands (when occupied) such that the conduction electrons can be treated as nonlocalized nearly free electrons; therefore, the electron-ion interaction in these metals can be represented by a pseudopotential, enabling one to perform rather easily accurate calculations of the average mass-enhancement coefficient λ. Successful calculations of the electron-phonon contribution to the mass enhancement in simple metals have been reported by several authors,[2] who have essentially used one or two orthogonalized plane waves (OPW's) and an isotropic approximation for the phonon spectrum. On the other hand, a general formulation to evaluate the electron-phonon matrix elements for more complex metals was discussed by Sinha[3] and Golibersuch[4] as early as 1968, and a phenomenological interpretation of the cyclotron-mass data by Lee[5] demonstrated the high anisotropy of the electron-phonon mass enhancement in Cu. However, until very recently, no detailed calculation of the electron-phonon–interaction matrix elements have been reported. Recently Allen and Lee[6] have extended the phase-shift model of calculating the Fermi-surface properties to express the matrix elements of the electron-phonon interaction in the augmented-plane-wave (APW) formalism given by Golibersuch.[4] This formulism uses the criteria discussed by Heine and Lee[7] for choosing the Fermi-energy parameter for calculating the phase shifts for electron-phonon–interaction matrix elements. Allen and Lee have successfully applied their model to the alkali-series metals. Independently, Chui[8] has also parameterized the APW formalism of Sinha[3] in terms of the d bandwidth and energy, but no rigorous application of his techniques has yet been reported. The first attempt to calculate the velocity-renormalization constant directly for copper, a metal with d bands lying close to the conduction bands, was done by Teichler,[9] who used the Wannier-function representation and a simplified model for the phonon-dispersion relation neglecting the phonon polarization. However, the results obtained were in poor qualitative agreement with the phenomenological results.[5] More recently, Nowak[10] has extended the formulation of Allen and Lee[6] to discuss the velocity renormalization and thermal phonon scattering in copper. He included the effects of the phonon polarization and umklapp processes. His results are in very good quantitative agreement with the ones obtained by Lee[5] for the anisotropic velocity renormalization and also with the recent experimental results on the quasiparticle scattering rate by Gantmakher[11] and Koch and Doezema.[12]

An alternative approach to the calculation of the electron-phonon–interaction matrix elements is presented taking into account explicitly all the necessary factors such as screening, the transverse and longitudinal phonons, the umklapp processes, and the band-structure effects.

The method discussed here differs from that of the other workers, with the exception of Nowak,[10] in that it neither has any adjustable parameters other than those previously used to form the band structure itself, nor does it derive the anisotropic mass renormalization through any comparative ratio. Hence, the successful application of this method to the calculation of the anisotropic velocity renormalization[5] and the quasiparticle scattering rate in copper[10] suggests that it can reliably be used to calculate the electron-phonon–interaction effects not only in the normal transition metals but also in the superconducting metals.

The general plan of the paper is as follows: In Sec. II the general calculation of the electron-phonon–interaction effects on the mass renormalization and the quasiparticle scattering time is discussed; in Sec. III band-structure calculations are reviewed briefly; in Sec. IV the calculation of the electron-phonon–interaction matrix elements is discussed; Sec. V contains details of the computational techniques employed; in Sec. VI the results obtained for copper using the above method are presented; and finally possible improvements and application of the method to other metals including the superconductors are discussed.

II. GENERAL FORMULATION OF CALCULATION OF ELECTRON-PHONON INTERACTION

The many-body effects of the Fermi velocities and the cyclotron masses can be taken into account approximately by expressing the one-electron propagator for the interacting system as

$$G(\vec{x},\vec{x}') = \sum_{\vec{k},n} \frac{\psi^{n*}_{\vec{k}}(\vec{x})\psi^{n}_{\vec{k}}(\vec{x}')}{\omega - \omega^n(\vec{k}) - \Sigma^n_{ee}(\vec{k},\omega) - \Sigma^n_{ep}(\vec{k},\omega)} \quad . \tag{1}$$

Thus the quasiparticle energy differs from the band-structure energy by the self-energies $\Sigma^n_{ee}(\vec{k},\omega)$, the contribution from the electron-electron interaction, and that from the electron-phonon contribution $\Sigma^n_{ep}(\vec{k},\omega)$. The self-energy Σ_{ep} influences the bands only near the Fermi surface, whereas Σ_{ee} modifies the band structure smoothly and therefore can be folded into a semiempirical one-electron potential. Thus the quasiparticle energy $\omega^n(\vec{k})$ for the nth band is given by

$$\omega^n(\vec{k}) = \omega^n_B(\vec{k}) + \mathrm{Re}\Sigma^n_{ep}(\vec{k},\omega)\big|_{\omega=\omega^n(\vec{k})} \quad , \tag{2}$$

where $\omega^n_B(\vec{k})$ is the band-structure energy that includes the electron-electron–interaction effects. One can relate the band-structure velocity $V^n_B(\vec{k})$ to the quasiparticle velocity $V^n(\vec{k})$ through the mass-enhancement factor $\lambda^n_{\vec{k}}$ as follows[13]:

$$V^n(\vec{k}) = \nabla_{\vec{k}}\omega^n(\vec{k}) = \frac{V_B^n(\vec{k})}{1-(\partial/\partial\omega)\,\mathrm{Re}\Sigma^n_{ep}(\vec{k},\omega)\,|_{\omega=\omega^n(\vec{k})}}$$

$$= \frac{V_B^n(\vec{k})}{1+\lambda^n_{\vec{k}}} \quad . \tag{3}$$

Here $V_B^n = \nabla_{\vec{k}}\omega_B^n(\vec{k})$ is the velocity derived from band-structure calculations, and $\lambda^n_{\vec{k}}$ is the velocity-renormalization constant at point $\vec{k}$. Considering only the lowest-order contribution to the self-energy from the electron-phonon interaction,[14] one gets

$$\Sigma^n_{ep}(\vec{k},\omega) = \frac{i\Omega_0}{(2\pi)^4} \times \int \sum_{\vec{q}\lambda n'} \frac{D_{\vec{q}\lambda}(\omega')\,|M^{nn'}_{\vec{k}\vec{k}'\lambda}(\vec{q})|^2}{\omega+\omega'-\omega^{n'}(k')+i\eta_{\vec{k}'}}\, d\vec{k}'\, d\omega \quad ,$$

where $D_{\vec{q}\lambda}(\omega) = 2\omega_{\vec{q}\lambda}/[\omega^2-(\omega_{\vec{q}\lambda}-i\delta)^2]$, $\omega_{\vec{q}\lambda}$ being the phonon energies

$$M^{nn'}_{\vec{k}\vec{k}'\lambda}(\vec{q}) = \langle\psi^n_{\vec{k}}|g_{\vec{q}\lambda}|\psi^{n'}_{\vec{k}'}\rangle = \left(\frac{\hbar}{2M\omega_{\vec{q}\lambda}\Omega_0}\right)^{1/2} \sum_\mu \langle\psi^n_{\vec{k}}|\vec{\nabla}V(\vec{r})|\psi^{n'}_{\vec{k}'}\rangle \times \vec{e}_{\vec{q}\lambda}\, e^{i\vec{q}\cdot\vec{R}^0_\mu} \sum_{G_p} \delta_{\vec{k}'-\vec{k},q+G_p} \quad . \tag{4}$$

Here summation over μ refers to only the ions in unit cell, and $V(\vec{r})$ denotes the screened potential at the point $\vec{r}$ due to the ions in the unit cell located at the origin:

$$V(\vec{r}) = \int \epsilon^{-1}(\vec{r},\vec{r}')V_c(\vec{r}')\,d^3r' \quad . \tag{5}$$

Carrying out the integration over $d\omega'$, one gets the velocity-renormalization factor

$$\lambda^n_{\vec{k}} = \frac{\Omega_0}{(2\pi)^3}\sum_{n'}\int \frac{d^3k'\sum_\lambda |M^{nn'}_{\vec{k}\vec{k}'\lambda}(\vec{q})|^2}{(\omega_{\vec{q}\lambda}+|E^{n'}_{\vec{k}'}-\epsilon_F|)^2} \quad , \tag{6}$$

where ϵ_F is the Fermi energy,

$$E^{n'}_{\vec{k}-\vec{q}} = \epsilon_F - \omega^{n'}(\vec{k}-\vec{q}),$$

and

$$\vec{k}-\vec{k}' = \vec{q}+C'_n \quad . \tag{7}$$

The vector $\vec{q}$ lies within the first Brillouin zone.

We shall also consider the relaxation time of the quasiparticle, which is obtained from a thermal average of the imaginary part of the self-energy (defined from the temperature-dependent electron-phonon Green's function). Thus the relaxation time $\tau^n_{\vec{k}}$ of the added electron at the point $\vec{k}$ in the band n is given by[10]

$$\frac{\hbar}{\tau^n_{\vec{k}}} = \sum_\lambda \frac{2K_B^3\Omega}{\pi M\hbar^3 V_{\vec{k}}}\,\frac{12}{7}\,\zeta(3)\left\langle\frac{|V^\lambda(0,\vec{k})|^2}{C_\lambda^4}\right\rangle T^3 \quad , \tag{8}$$

where K_B is the Boltzmann constant, $\zeta(3)$ is the Rieman ζ function, C_λ is the velocity of sound for polarization λ, and $\langle|V^\lambda(0,\vec{k})|^2/C_\lambda^4\rangle$ denotes the angular average of the quantity

$$\frac{|V^\lambda(0,\vec{k})|^2}{C_\lambda^4} = \lim_{\vec{k}'\to\vec{k}} \frac{2M|\vec{k}-\vec{k}'|^2}{\hbar\omega^3_{\vec{q}\lambda}} \sum_{n'} |M^{nn'}_{\vec{k}\vec{k}'\lambda}(\vec{q})|^2 \quad . \tag{9}$$

The following major steps are included in the calculation of $\lambda^n_{\vec{k}}$ and $\tau^n_{\vec{k}}$: (i) calculation of the band structure, the density of states, the value of the Fermi energy, and expressions for the wave function and energy at a general point; (ii) calculation of the dispersion relation for phonons; (iii) calculation of the electron-phonon–interaction matrix elements for the transition from state $\psi^n_{\vec{k}}$ to $\psi^{n'}_{\vec{k}'}$ with momentum transfer $\vec{q}$; and (iv) evaluation of the integral (6) over $\vec{k}'$ on the Fermi surface finally gives the velocity renormalization constant $\lambda^n_{\vec{k}}$. These steps will now be described in relation to copper in the following sections.

III. BAND-STRUCTURE CALCULATIONS

In the formalism presented here the Bloch functions $\psi^n_{\vec{k}}$ are expressed as a linear combination of OPW's and the tight-binding d states in the same manner as in the combined interpolation scheme.[15] The approach modifies the latter to make it suitable for the calculation of the electron-phonon–interaction matrix elements. In order to include the effect of the umklapp processes properly, the OPW basis set was augmented from 4 OPW's to 15 OPW's, which include the first three stars of the reciprocal-lattice vectors, so that all the portions of the Brillouin zone were treated on the same footing and it was possible to consider the transformation properties of the matrix elements properly. Thus the wave function ψ^n_k can be represented by

$$\Psi^n_{\vec{k}}(\vec{r}) = \sum_{\substack{H\\ \text{first}\\ \text{three}\\ \text{stars}}} C^n_{\vec{k}+\vec{H}}\,\Psi_{\vec{k}+\vec{H}}(\vec{r}) + \sum_m D^n_{m\vec{k}}\varphi^{\vec{k}}_{dm}(\vec{r}) \quad , \tag{10}$$

where

$$\Psi_{\vec{k}+\vec{H}}(\vec{r}) = \frac{1}{c_{\vec{k}+\vec{H}}}\left(|\vec{k}+\vec{H}\rangle - \sum_m \langle\varphi^{\vec{k}}_{dm}|\vec{k}+\vec{H}\rangle|\varphi^{\vec{k}}_{dm}\rangle\right) \quad ,$$

$$c_{\vec{k}+\vec{H}} = \left(1-\sum_m |\langle\varphi^{\vec{k}}_{dm}|\vec{k}+\vec{H}\rangle|^2\right)^{1/2} \quad , \tag{11}$$

$$\varphi^{\vec{k}}_{dm}(\vec{r}) = \sum_{\substack{R\\ \text{nearest}\\ \text{neighbors}}} e^{i\vec{k}\cdot\vec{R}}\varphi_{dm}(\vec{r}-\vec{R}) \quad .$$

Before discussing the details of the derivation of the wave function, a few comments shall be made about the orthogonality to core functions and its contribution to electron-phonon matrix elements.

Since in the formulation the effect of s and p core states has been folded into the potential with the help of the pseudopotential formulation in the

interpolation scheme, the wave function obtained could be considered to be the true wave function if the basis set were complete. Since this is not strictly true, it is in principle necessary to orthogonalize the interpolation-scheme wave function to the core s and p states. However, it shall be shown that the correction to the electron-phonon-interaction matrix elements due to this orthogonalization effect is negligible. This is because the s and p core states are extremely localized, and therefore most of their contribution to the matrix elements comes from the small values.

The matrix elements of the electron-phonon interaction between the states $\Psi^n_{\vec{k}}$ and $\Psi^n_{\vec{k}'}$ can be written

$$\langle \Psi^n_{\vec{k}} | \nabla V | \Psi^n_{\vec{k}'} \rangle = \frac{1}{N_{\vec{k}} N_{\vec{k}'}} \Big(\langle \Psi^I_{\vec{k}} | \nabla V | \Psi^I_{\vec{k}'} \rangle - \sum_c \langle \Psi^I_{\vec{k}} | \Psi^c_{\vec{k}} \rangle \times \langle \Psi^c_{\vec{k}} | \nabla V | \varphi^I_{\vec{k}'} \rangle - \sum_c \langle \Psi^I_{\vec{k}} | \nabla V | \Psi^c_{\vec{k}'} \rangle \langle \Psi^c_{\vec{k}'} | \Psi^I_{\vec{k}'} \rangle + \sum_{cc'} \langle \Psi^I_{\vec{k}} | \Psi^c_{\vec{k}} \rangle \langle \Psi^{c'}_{\vec{k}'} | \Psi^I_{\vec{k}'} \rangle \langle \Psi^c_{\vec{k}} | \nabla V | \Psi^{c'}_{\vec{k}'} \rangle \Big) \quad , \tag{12}$$

where $\Psi^I_{\vec{k}}$ is the wave function obtained from the interpolation scheme and $\Psi^c_{\vec{k}}$ the tight-binding function obtained from the core state ψ_c. The summation over core states involves the $1s$, $2s$, $2p$, $3s$, and $3p$ states, and $N_{\vec{k}}$ and $N_{\vec{k}'}$ are the normalization constants. The effect of the orthogonalization of the wave function is essentially to replace the Fourier transform of the crystal potential $V(r)$ by a pseudopotential $V(r) + V_R(r, r')$, the corresponding additional contribution to the electron-phonon matrix elements being[16]

$$\left(\frac{\hbar}{2M\omega_{\vec{q}\lambda}\Omega_0} \right)^{1/2} \sum_t (E^n_{\vec{k}} - \epsilon_t) b^*_{t\vec{k}} b_{t\vec{k}'} \vec{e}_{\vec{q}\lambda} \cdot (\vec{k} - \vec{k}') \quad , \tag{13}$$

where ϵ_t is the energy and $b_{t\vec{k}}$ the Fourier transform of the core orbital ψ_t. It is found that this term is of the order of 1% of the matrix element obtained without the orthogonalization. Thus it is justified to neglect the corrections due to explicit orthogonalization of the interpolation-scheme functions to the core states.

We will not discuss here the details of the band-structure calculations, as they are already given by Mueller.[15] However, we will present the features of our method which differ from those described by Mueller.

(a) Here the effect of the second nearest neighbors, which was neglected originally, has been included.

(b) A better representation of the form factor $f(k)$, which enters in the overlap between the plane waves and the tight-binding d functions, has been considered. In the original calculations, the overlap was represented by

$$\varphi_{dm}(\vec{k}) \equiv \langle \varphi^{\vec{k}}_{dm} | \vec{k} \rangle = A_0 Y_{2m}(\hat{k}) j_2(kR_0) = Y_{2m}(\hat{k}) f(k) \quad ,$$

where the parameters A_0 and R_0 were determined by making the least-squares fit to the eigenvalues obtained from the APW method. Also an arbitrary cutoff was introduced in $f(k)$ at the first node of $j_2(kR_0)$. Although Mueller was successful in parametrizing the Hamiltonian to get a good fit to the APW eigenvalues, his method could not decide the form of the function $f(k)$ for large k values. Also the accuracy of wave functions obtained from the combined interpolation scheme is difficult to assess. When we applied the combined interpolation scheme to calculate the positron-annihilation spectra in palladium,[17] it was found that the disagreement with the experimental results could be reduced by modifying the form factor $f(k)$ [as the disagreement was occurring at the values of kR_0 where we introduced the cutoff in $j_2(kR_9)$]. To avoid this, we used the Slater-type expansion for the $3d$ atomic functions for copper. It is found by Lipari and Deegan[18] that the optimized wave functions for $3d$ electrons of copper with Chodorow's[19] potential represent quite satisfactorily the band structure of copper. The three d-band parameters—$dd\sigma$, $dd\pi$, and $dd\delta$—calculated by Lipari and Deegan[18] are listed along with the values from the present work in Table I. We have represented the d function by

$$\varphi_{dm}(\vec{r}) = \sum_p c_p A_p r^2 e^{-\xi_p r} Y_{2m}(\hat{r}) \quad , \qquad A_p = (2\xi_p)^{7/2} (6!)^{-1/2} \quad . \tag{14}$$

The values of the parameters ξ_p and c_p were taken from the atomic calculations of Wahl *et al.*[20]

It was found that use of Lipari and Deegan's[18] values of $dd\sigma$, $dd\pi$, and $dd\delta$, in place of those obtained from the least-squares fit to the APW, eigenvalues at high-symmetry points, changed the energy eigenvalues by only a few millirydbergs near the Fermi energy; the changes in the values

TABLE I. First-neighbor linear-combination-of-atomic-orbitals parameters (in Ry) for copper in the two-center approximation.

Parameter	Combined[a] interpolation scheme	Lipari and Deegan[b]	Present interpolation scheme	Slater-type atomic orbitals for Cu $3d$ state
$dd\sigma$	−0.0257	−0.021 26	−0.0258	−0.0188
$dd\pi$	0.0132	0.009 40	0.0139	0.0104
$dd\delta$	−0.0014	−0.000 88	−0.0017	−0.0018

[a]Reference 15. These parameters were obtained by fitting the band structure of Burdick, who has used Chodorow's potential.

[b]Reference 18.

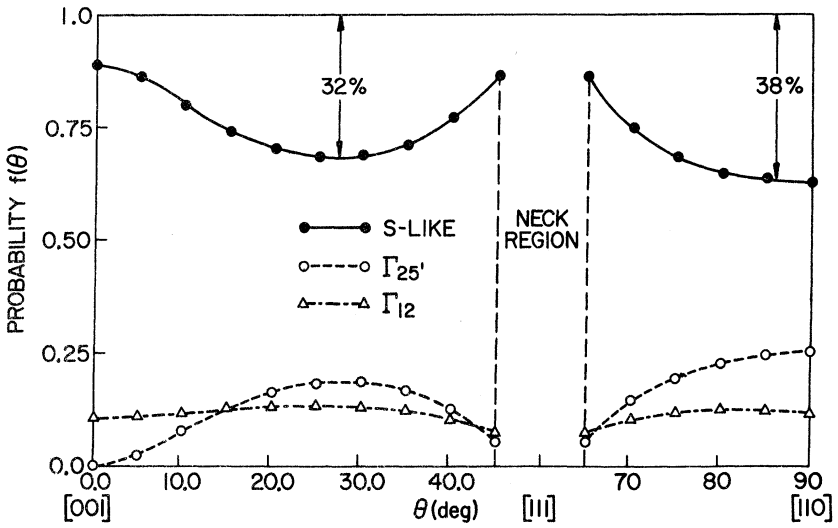

FIG. 1. Angular variation of the character of the eigenfunctions on the Fermi surface of copper in [110] plane. The plane-wave (s) and $d-(\Gamma_{25}', \Gamma_{12})$ probabilities $f(\theta)$, θ being measured from (001) direction, are given by the squares of the respective amplitudes in the sixth-band state of copper. The d-function character has a maximum of 38% along [110] direction.

of matrix elements $M_{\vec{k}\vec{k}'\lambda}^{nn'}(\vec{q})$ on the Fermi surface were also less than 5%. On the other hand, when values were obtained for $dd\sigma$, $dd\pi$, and $dd\delta$ by using wave functions represented by Eq. (14), it was found that though the energy eigenvalues changed by only a few millirydbergs, i.e., an amount within the limits of accuracy given by the interpolation scheme, the changes in the matrix elements were slightly more than those given by Lipari's values for d-band parameters, being consistently less than 8%. Because the wave function obtained by Lipari and Deegan[18] is not very different from the one given by the Slater-type expansion form, we have decided to use the latter representation for the atomic d functions in the tight-binding representation of the crystal wave functions for preliminary calculations to verify our formulation. We have also studied the character of the eigenfunctions on the Fermi surface of copper in the (110) plane. The results are shown in Fig. 1, where the probability of a given symmetry character is the sum of the squares of the amplitudes of the corresponding basis functions. The d character is maximum along the [110] direction where it is only 38%; consequently, a slight error in representing the d bands should not cause more than 5% error in the matrix elements of the electron-phonon interaction.[21] The values of the parameters used to parametrize the Hamiltonian are listed in Table II.

IV. ELECTRON-PHONON-INTERACTION MATRIX ELEMENTS

In the present formalism, the Bloch functions $\Psi_{\vec{k}}^{n}$ are expressed as a linear combination of the OPW's and the tight-binding d states. The matrix elements $M_{\vec{k}\vec{k}'\lambda}^{nn'}(\vec{q})$ will, therefore, involve the three types of terms: those between the plane waves, those between the plane wave and d states, and those between the d states. The matrix elements between the plane-wave states $\vec{k}$, $\vec{k}'$ are simply given by

$$\langle\vec{k}|g_{\vec{q}\lambda}(\vec{r})|\vec{k}'\rangle=\left(\frac{\hbar}{2M\Omega_0\omega_{\vec{q}\lambda}}\right)^{1/2}\times\frac{V_c(|\vec{k}'-\vec{k}|)}{\epsilon(|\vec{k}'-\vec{k}|,0)}\,(\vec{k}'-\vec{k})\cdot\vec{e}_{\vec{q}\lambda}\ , \quad (15)$$

where $V_c(\vec{q})$ is the Fourier transform of the ionic potential $V_c(\vec{r})$ (which has been taken for copper to

TABLE II. Values of interpolation-scheme parameters chosen for the copper band structure.[a]

	Parameter	Parameter values (Ry)
d bands	d_0	−0.6107
	$dd\sigma$	−0.0258
	$dd\pi_1$	0.0139
	$dd\delta$	−0.0017
	γ	0.0017
d bandwidth	W	0.9964
Conduction bands	V_{111}	0.005
	V_{200}	0.0339
Orthogonality	A	1.0163
	LR_0	2.9958
Hybridization	B	1.299
	LR_1	3.0394
Second-neighbor parameters	$(dd\pi)$	0.0003
	$(dd\delta)$	0.0001
	$(dd\sigma)$	−0.0019
Fermi energy	E_F	0.5685
Deviation of fit	$D(P)$	0.006

[a]For the definition of the parameters, see Ref. 32.

be of Chodorow's form[19], and $\epsilon(q,0)$ is the static dielectric constant for wave vector q (approximated in this case by Lindhard's function[14]). For the terms involving $\langle\varphi^{\vec{k}}_{dm}|g_{\vec{q}\lambda}(\vec{r})|\vec{k}'\rangle$, we neglect the overlap terms obtaining

$$\langle\varphi^{\vec{k}}_{dm}|g_{\vec{q}\lambda}(\vec{r})|\vec{k}'\rangle = \frac{1}{(2\pi)^3}\left(\frac{\hbar}{2M\omega_{\vec{q}\lambda}\Omega_0}\right)^{1/2} \times\int \varphi_{dm}(\vec{k}'-\vec{q}')\vec{q}'\cdot\vec{e}_{\vec{q}\lambda}\,\frac{V_c(q')}{\epsilon(q,0)}\,d^3\vec{q}' \,, \tag{16}$$

where $\varphi_{dm}(\vec{q})$ is the Fourier transform of the atomic function $\varphi_{dm}(\vec{r})$ defined by Eq. (14). Thus,

$$\varphi_{dm}(\vec{q}) = Y_{2m}(\hat{q})f(q) \,,$$
$$f(q) = \sum_p A_p C_p \int r^4 e^{-\xi_p r} j_2(qr)\,dr \,. \tag{17}$$

When all overlap contributions are neglected, the electron-phonon matrix elements between the tight-binding d functions are identically zero. To determine the form of the d-d contribution, we next consider the approximations in which the two-center terms (arising from d-d overlap) and the degenerate three-center terms (arising from the overlap of the potential with the d functions centered on nearest-neighbor sites) were retained. The d-d matrix elements in this approximation are of the form (Appendix A)

$$\langle\varphi^{\vec{k}}_{dm}|g_{\vec{q}\lambda}(r)|\varphi^{\vec{k}'}_{dm}\rangle = \frac{1}{(2\pi)^3}\left(\frac{\hbar}{4M\omega_{\vec{q}\lambda}\Omega_0}\right)^{1/2} \sum_{\substack{R\\ \text{nearest}\\ \text{neighbors}}} e^{i\vec{q}\cdot\vec{R}} \sum_{\substack{L=0,2,4\\ l=1,3,5\\ M=1,0,1}} (4\pi)^2(2L+1)^{1/2}(2l+1)^{-1/2}(i)^{L+l+1}C(2,L,2;m,m'-m)$$
$$\times C(2,L,2;0,0)C(1,L,l;M,m'-m)C(1,L,l;0,0)Y_{lm'-m+M}(\hat{R})F_{Ll}D^M_{\vec{q}\lambda}$$
$$+\frac{1}{2\pi^2}\left(\frac{\hbar}{4M\omega_{\vec{q}\lambda}\Omega_0}\right)^{1/2}\sum_R\left[e^{i\vec{k}\cdot\vec{R}}I_{\vec{q},mm'}(\vec{R})+e^{-i\vec{k}\cdot\vec{R}}I^*_{\vec{q},mm'}(\vec{R})\right] \,, \tag{18}$$

where

$$I_{\vec{q},mm'}(\vec{R}) = \sum_{\substack{l=0,1,\ldots,5\\ 2\geq t\geq|\mu|\\ M=-1,0,1}}\left(\frac{4\pi(2t+1)}{5(2l+1)}\right)^{1/2}B_{m't\mu}(\vec{R})Y^*_{lm-\mu-M}(\vec{R})S_{lt}(R)D^M_{\vec{q}\lambda}\sum_{\substack{L=0,2\text{ for }t=1\\ L=1,3,\ldots(t+1)\text{ for }t\text{ even}}} C(t,1,L;\mu,M)C(t,1,L;0,0)$$
$$\times C(l,L,2;m-\mu-M,\mu+M)C(l,L,2;0,0) \,,$$
$$F_{Ll} = \int_0^\infty q'^3\,\frac{V_c(q')}{\epsilon(q',0)}\,j_l(q'R)f_L(q')\,dq' \,,$$
$$f_L(q') = \left(\frac{2L+1}{4\pi}\right)^{1/2}\sum_{st} C_sC_tA_sA_t\int_0^\infty r^6 j_L(q'r)\,e^{-(\xi_s+\xi_t)r}\,dr \,,$$
$$D^1_{\vec{q}\lambda} = -(\vec{e}_{\vec{q}\lambda x}-i\vec{e}_{\vec{q}\lambda y}),\quad D^{-1}_{\vec{q}\lambda} = (\vec{e}_{\vec{q}\lambda x}+i\vec{e}_{\vec{q}\lambda y}),\quad D^0_{\vec{q}\lambda} = \sqrt{2}\,\vec{e}_{\vec{q}\lambda z} \,, \tag{19}$$
$$S_{lt}(R) = \sum_{pq}A_pA_qC_pC_q\int_0^\infty w(r)f_l(\xi_p r_<,\xi_p r_>)e^{-\xi_q r}r^{4+t}R^{2-t}\,dt \,,$$
$$w(r) = 2\pi^2\frac{dV}{dr} = \int_0^\infty \frac{q^3 j_1(qr)V_c(q)}{\epsilon(q,0)}\,dq \,.$$

$V(r)$ is the screened ionic potential, and $f_l(\xi_p r_<, \xi_p r_>)$ are the functions of the Bessel functions of imaginary argument and half-integral order and are discussed in Appendix A. The quantities $\vec{e}_{\vec{q}\lambda x}$, $\vec{e}_{\vec{q}\lambda y}$, and $\vec{e}_{\vec{q}\lambda z}$ are the x, y, and z components of the phonon-polarization vectors $\vec{e}_{\vec{q}\lambda}$. The form factors $f(q)$, $f_0(q)$, $f_2(q)$, and $f_4(q)$ are plotted in Fig. 2. The first term in Eq. (18) represent the contribution from the degenerate three-center-type terms while the second represents the contribution from the two-center-type terms.

The derivation of $B_{mt\mu}(\hat{R})$ is discussed in Appendix B (the constants are tabulated in Table III) and can be used for any lattice structure as the direction of R is completely arbitrary. We believe that the contribution from the three-center term is negligible for reasons explained later.

The choice of potential used for the first-principles calculations of the electron-phonon interaction is still a point of discussion.[22] We think that the screened Chodorow's atomic potential is at the very least a reasonable choice of potential for the

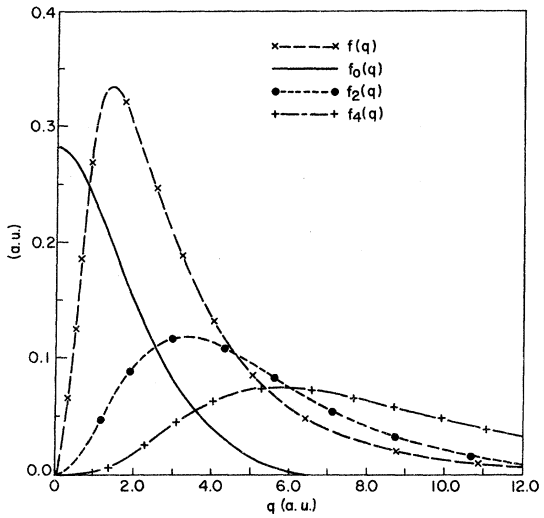

FIG. 2. Radial form factors for d states: The form factor $f(q)$ is the fourier transform of radial part of $\varphi_{dm}(\vec{r})$; $f_0(q)$, $f_2(q)$, and $f_4(q)$ are related to the Fourier transforms of $\varphi^2_{dm}(\vec{r})$. The long tail in the form factors beyond $q=2k_F$ (1.5 a.u.) demonstrates the importance of the umklapp processes in the electron-phonon interaction.

following reasons. Since copper has d bands lying very close to the conduction band, the assumption that the d electrons are tightly bound to the ion and hence move rigidly with it, when displaced, is clearly not correct; consequently, the validity of linear screening via Lindhard's dielectric function (which is obtained in the free-electron approximation from the requirement of self-consistency of the potential with respect to the displaced charge cloud) becomes rather doubtful. However, since the screening effects are to be considered only at large distance from the nucleus where the d part of the conduction-band states is weak, Lindhard's screening should be approximately valid. It is assumed that the potential is given correctly by Chodorow's form inside the muffin-tin sphere, while it goes as $\approx -2/r$ (in Ry) outside the muffin-tin sphere. The Fourier transform of this potential screened by Lindhard's dielectric function $[V_{CM}/\epsilon(q,0)]$ is shown in Fig. 3. The Fourier transform of Chodorow's potential screened with Lindhard's dielectric function $[V_C/\epsilon(q,0)]$ (but with the assumption that the potential outside the muffin-tin sphere is essentially constant) is also shown in the same figure, and it is clear that the two curves differ from each other only in the small-q region of 0.3 a.u. Since the contribution of the umklapp processes to the matrix elements is also very important, the contribution from the phonons of large wavelengths to the mass-renormalization constants $\lambda^n_{\vec{k}}$ is not very important. Thus one is justified in taking the gradient of the potential outside the muffin-tin sphere as essentially zero for the calculations of the $\lambda^n_{\vec{k}}$. It is shown by Lee[23] that Chodorow's potential reproduces the Fermi-surface properties quite accurately and that the correction to this potential due to nonlocality is also very small.

TABLE III. Constants $B_{mt\mu}(\hat{R})$ occurring in the tight-binding electron-phonon–interaction matrix elements. [Note that when $m=-1$ or -2, only negative values of μ contribute and $Y_{tm}(\theta_R,\varphi_R)$ in the table is replaced by the corresponding $Y_{t-m}(\theta_R,\varphi_R)$. $B_{mt\mu}=0$ for μ negative and m positive.]

	μ	$t=0$	1	2
$m=0$	0	$[(1/4\pi)Y_{20}(\theta_R,\varphi_R)]^{1/2}$	$-[\frac{80}{9}\pi Y_{10}(\theta_R,\varphi_R)]^{1/2}$	1
	1	0	$[\frac{80}{9}\pi Y^*_{11}(\theta_R,\varphi_R)]^{1/2}$	0
	2	0	0	0
$m=1$	0	$[(1/4\pi)Y_{21}(\theta_R,\varphi_R)]^{1/2}$	$[\frac{80}{9}\pi Y_{11}(\theta_R,\varphi_R)]^{1/2}$	0
	1	0	$-[\frac{80}{9}\pi Y_{10}(\theta_R,\varphi_R)]^{1/2}$	1
	2	0	0	0
$m=2$	0	$[(1/4\pi)Y_{22}(\theta_R,\varphi_R)]^{1/2}$	0	0
	1	0	$-[\frac{40}{9}\pi Y_{11}(\theta_R,\varphi_R)]^{1/2}$	0
	2	0	0	0

V. COMPUTATIONAL TECHNIQUES

The calculation of the velocity-renormalization factors $\lambda^n_{\vec{k}}$ and the scattering rates of the quasiparticle $\tau^n_{\vec{k}}$ involve the following three major steps.

A. Calculation of Energy - Band Structure

The interpolation-scheme formalism discussed by Mueller[15] has been followed for calculating the

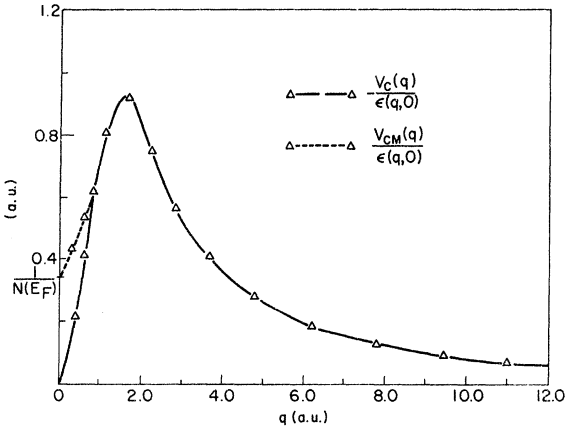

FIG. 3. Fourier transform of Chodorow's potential screened by Lindhard's dielectric function. Whereas $V_c(r)$ is assumed to have zero gradient outside the muffin-tin sphere, the modified form $V_{CM}(r)$ goes as $-2/r$ (Ry) outside the muffin-tin radius, and $V_{CM}(q)/\epsilon(q,0)$ leads to the correct long-wavelength limit $1/N(E_F)=0.285$ Ry.

TABLE IV. Atomic force constants used in the calculations of the phonon-dispersion relation for copper.[a]

Atomic force	Constants dyn/cm
φ_{xx}^1	13 102
φ_{zz}^1	−1 417
φ_{xy}^1	14 820
φ_{xx}^2	361
φ_{yy}^2	−238
φ_{xx}^3	642
φ_{yy}^3	315
φ_{yz}^3	190
φ_{xz}^3	385
φ_{xx}^4	104
φ_{zz}^4	−284
φ_{xy}^4	396
φ_{xx}^5	−137
φ_{yy}^5	9
φ_{zz}^5	−16
φ_{xy}^5	−55
φ_{xx}^6	−138
φ_{yz}^6	−232

[a]Reference 25.

band structure of copper, and then the QUAD[24] scheme for determining the Fermi energy was used.

B. Evaluation of Matrix Elements $M^{nn'}_{\vec{k}\vec{k}'\lambda}(\vec{q})$

The calculation of the matrix elements involves essentially the computation of the form factors $f(q)$ and $f_L(q)$, the Fourier transform of the potential, $V_c(q)$, and the dielectric constant $\epsilon(q, 0)$. The dielectric function $\epsilon(q, 0)$ is assumed to be of Lindhard's form[14] and is given by

$$\epsilon(q, 0) = 1 + [4\pi e^2 N(\epsilon_F)/q^2]L(Q) \ ,$$

where $N(E_F)$ is the density of states at the Fermi energy and

$$L(Q) = \frac{1}{2}\left(1 + \frac{1-Q^2}{2Q}\ln\frac{1+Q}{1-Q}\right) \ , \qquad (20)$$

$$Q = q/2k_F \ .$$

Here k_F represents the free-electron Fermi radius for copper and is taken to 6.52 in $\pi/4a$ units, a being the lattice constant.

Another important quantity that is involved in the matrix elements is the phonon-dispersion relation, which was calculated using a Born–von Karman atomic-force-constant-dependent model. The model takes into account six shells of nearest neighbors. The parameters were determined from the inelastic-neutron-scattering data along the principal-symmetry directions,[25] and are given in Table IV.

It has been assumed, as in the usual band-structure calculations, that the potential outside the muffin-tin radius is constant, and the constant quantity V_{MT}, the potential at the muffin-tin radius, has then been subtracted from Chodorow's potential on calculating the Fourier transform of the potential V_c. Thus the gradient of the potential is essentially zero outside the muffin-tin radius for V_c.

The contribution from umklapp processes enters into the expression for the matrix elements $M^{nn'}_{\vec{k}\vec{k}'\lambda}(q)$ in our formalism in a natural way since the basis set representing the wave function $\Psi^n_{\vec{k}}$ includes higher OPW's too.

Owing to the high symmetry of the points selected for calculating the mass-renormalization constant $\lambda^n_{\vec{k}}$, it was possible to reduce drastically the number of matrix elements that had actually to be computed. Group-theoretical transformations on the eigenvectors were then used to obtain the rest of the relevant matrix elements resulting in considerable saving of computer time.

C. Calculation of $\lambda^n_{\vec{k}}$ and $\tau^n_{\vec{k}}$

As was mentioned earlier, the major contribution to the integrals for $\lambda^n_{\vec{k}}$ and $\tau^n_{\vec{k}}$ comes from the transition from the states near the Fermi surface. To evaluate these integrals, a technique similar to the QUAD technique discussed by Mueller *et al.*[24] was followed. First the double Brillouin zone was divided into small cubical boxes as in the QUAD scheme and then the contributions to these integrals considered from only those boxes that enclosed portions of the sixth-band Fermi surface of copper. For each of these latter boxes a quadratic-interpolation fit of the quantities $|M^{nn'}_{\vec{k}\vec{k}'\lambda}(\vec{q})|^2/\omega^2_{\vec{q}\lambda}$, $\omega_{\vec{q}\lambda}$, and $E^n(\vec{k}')$ was derived. Unlike the QUAD scheme, however, a three-dimensional quadratic-interpolation scheme was adopted, in which for every set of (q_x, q_y) values a different parabolic fit is performed over three q_z values. This considerably reduced the rms error of the least-squares fit, being consistently about 5% for the mesh size equal to four. The Diophantine method is then used to calculate the integrals in Eqs. (8) and (9) with 15 000 points for every box. Owing to the well-behaved nature of the integrand, the statistical error is less than 0.01%. In this procedure it was sufficient to calculate the matrix elements at only 70 independent points for each value of k; and out of the 64 cubes into which the positive octant of the Brillouin zone was divided, it was necessary to consider only 16 in the calculations of $\lambda^n_{\vec{k}}$.

VI. RESULTS AND CONCLUSIONS

In Fig. 4 $|g_{\vec{k}\vec{k}'}|^2$ (defined below) was plotted for three values of $\vec{k}$ [with $\vec{k}'$ varying on the (110) zone of the copper Fermi surface] for two different cases. In the first case, we consider only the contribution (represented by solid lines) from the plane wave of $\psi^n_{\vec{k}}$ and $\psi^n_{\vec{k}'}$ to $|g_{\vec{k}\vec{k}'}|^2$ given by

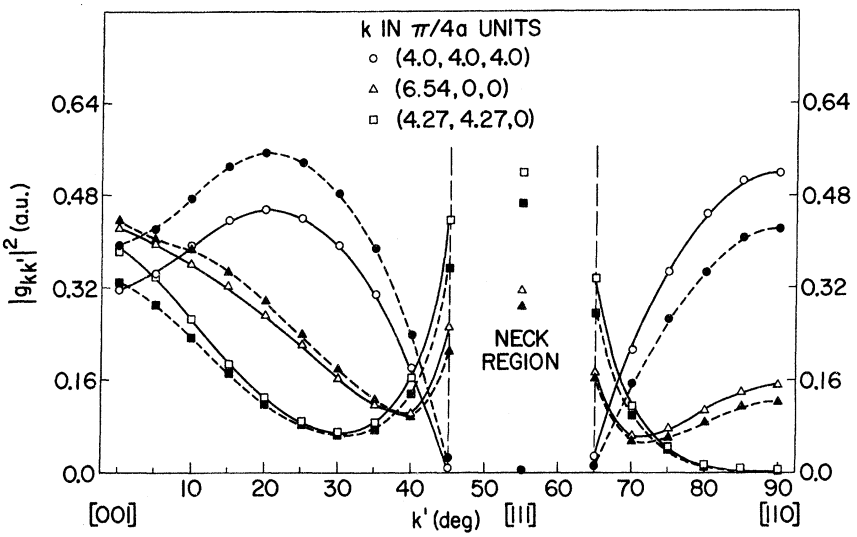

FIG. 4. Variation of the coupling constant $|g_{kk'}|^2$ on the Fermi surface. The point $\vec{k}'$ lies in the (110) plane and is given in terms of the angle measured from the Z direction. The point $\vec{k}$ lies on the high-symmetry directions indicated. The solid lines (with open symbols) represent the contribution from the plane-wave states only; whereas the dotted lines (with closed symbols) represent the total contributions including those from the d states.

$$|g_{\vec{k}\vec{k}'}|^2 = \sum_{\lambda} |\langle \psi^n_{\vec{k}} | e_{\vec{q}\lambda} \cdot \nabla V(\vec{r}) | \psi^n_{\vec{k}'} \rangle|^2 \ , \qquad (21)$$

whereas in the second case we consider, in addition to this, the contribution (represented by dotted lines) from the d state also.

With the present choice of potential (viz., that of Chodorow[19]), it is found that the value of integrals F_{Ll} and S_{lt} defined in Eq. (19) in atomic units is about 10^{-2} (see Tables V and VI) and the d-d matrix elements are, in general, smaller in magnitude than the matrix elements between the d states and the plane waves by at least one order of magnitude. Thus we are justified in completely neglecting the d-d part of the electron-phonon matrix elements. We must, however, point out that with other choices of potential, and/or when the wave function has considerable d character, this simplification may no longer be possible.

Thus we observe from Fig. 4 that the matrix elements are highly anisotropic. The anisotropy observed in the matrix elements could be observed only because we have considered explicitly the various factors like the phonon-polarization effects, the umklapp processes, the contribution from s-d hybridization, etc. In contrast to the assumption made by several workers[2,9] that most of the contribution to the electron-phonon matrix elements comes from the longitudinal phonons, Table VII shows that the transverse phonons are equally important in the electron-phonon interaction in copper. Indeed the main reason for the discrepancies between experimental and Teichler's result is that he considered only contributions from the longitudinal phonons. The results here agree with those of Nowak in showing that it is essential to consider the transverse phonons, particularly for the transition metals. The long tail in the form factors $f(q)$, $f_L(q)$, and the screened potential $V_c(q)/\epsilon(q, 0)$ (see Figs. 2 and 3) shows clearly that the umklapp processes are at least as important as the normal processes.

The results obtained by applying our formalism for $\lambda_{\vec{k}}$ and $\tau_{\vec{k}}$ along symmetry directions are given in Table VIII and show clearly the trend predicted by Lee, based on a phenomenological interpretation of the cyclotron-mass data, and agree very well with the results obtained by Nowak.[10] As explained below, this is due to the same physical basis of the two calculations. Nowak has suggested two possible explanations for the discrepancy between his results for the velocity-renormalization factor along the [110] direction (which are almost identical to ours) and the experimentally derived

TABLE V. Constants $10^2 F_{Ll}$ for copper using Chodorow's potential (in a.u.).

l \ L	0	2	4
1	−0.0012	0.0028	−0.0030
3	−0.4971	−0.0069	0.0005
5	−1.2340	−0.2322	0.0017

TABLE VI. Constants $10^2 S_{lt}(|R|)$ calculated for copper using Chodorow's potential (R is the nearest-neighbor distance in a.u.: $R = 6.83087/\sqrt{2} = 4.8304$).

l \ t	0	1	2
0	−0.8143	−0.0558	−0.0127
1	−0.1400	−0.0307	−0.0078
2	−0.0559	−0.0142	−0.0038
3	−0.0216	−0.0059	−0.0015
4	−0.0080	−0.0021	−0.0003
5	−0.0027	−0.0005	−0.0008

TABLE VII. Contribution from the transverse and longitudinal phonons to electron-phonon matrix elements $6.25\,|g_{\vec{K}\vec{K}'}|^2$ (a.u.) for copper.

K (in $\pi/4a$)	K' (in $\pi/4a$)	Longitudinal phonons	Transverse phonons
(4.0, 4.0, 4.0)	(4.364, 4.364, 2.877)	0.0275	0.0589
(6.54, 0.0, 0.0)	(4.364, 4.364, 2.877)	0.1648	0.8664
(4.27, 4.27, 0.0)	(4.364, 4.364, 2.877)	0.5484	1.180
(4.00, 4.00, 4.0)	(4.263, 4.263, 0.5272)	0.2064	2.3357
(6.54, 0.0, 0.0)	(4.263, 4.263, 0.5272)	0.3753	0.3420
(4.27, 4.27, 0.0)	(4.263, 4.263, 0.5272)	0.0096	0.01186
(4.0, 4.0, 4.0)	(4.246, 4.246, 1.0583)	0.1371	2.0603
(6.54, 0.0, 0.0)	(4.246, 4.246, 1.0583)	0.3615	0.1853
(4.27, 4.27, 0.0)	(4.246, 4.246, 1.0583)	0.0355	0.0300
(4.0, 4.0, 4.0)	(3.469, 3.469, 4.905)	0.0083	0.0983
(6.54, 0.0, 0.0)	(3.469, 3.469, 4.905)	0.1521	1.1522
(4.27, 4.27, 0.0)	(3.469, 3.469, 4.905)	0.0682	2.2437
(4.0, 4.0, 4.0)	(1.832, 1.832, 5.557)	0.3578	2.9947
(6.54, 0.0, 0.0)	(1.832, 1.832, 5.557)	0.9936	0.5227
(4.27, 4.27, 0.0)	(1.832, 1.832, 5.557)	0.4023	0.1142

value of Lee.[5] He points out, following Christensen,[13] that it is possible "that the Chodorow potential may be less than fully renormalized by the electron-electron interaction. If this is so, Lee's calculation might underestimate $\lambda(\vec{k})$. It is also possible that the discrepancies noted above could arise from uncertainties in the interpolation of the experimental data along various orbits to yield local values of the "quasiparticle velocity." However, we think the discrepancy between our results and those of Lee[5] and the excessively small d-d contribution to our electron-phonon interaction matrix elements can be attributed to the following possible sources of error in our calculation: (a) The potential experienced by electrons in the presence of lattice vibrations cannot strictly be taken in the form given by Chodorow.[26] The fact that the potential is not in general, spherically symmetric in the muffin-tin region is also a possible source of error. As has been mentioned by Barisic,[27] the rigid-ion approximation is less accurate for highly localized d states than for free electrons; in the tight-binding d-d matrix element the error is more than that in the matrix elements between the plane waves or between the plane-wave and d states. (b) The possible error from the atomic Slater-type expansion used for the functions $\varphi_{dm}(\vec{r})$ should also be considered. It is conceivable that crystal-optimized functions constructed to match the APW functions may lead to significant improvements. (c) Finally, Lindhard's approximation for the dielectric function is strictly valid only for free electrons, although it is reasonable to assume that this assumption has not introduced substantial error because of the over-all small d character on the Fermi surface of copper.

We shall comment briefly on the differences between the recent work on the electron-phonon interaction in copper by Nowak and the present work. Nowak's approach is an extension of the phase-shift description of the electron-phonon interaction in the alkali metals discussed by Allen and Lee,[6] which is based on Golibersuch's[4] formalism. In Nowak's approach, the self-consistency of the charge distribution is taken into account empirically by adjusting the Fermi-energy parameter to satisfy the long-wavelength limit of the pseudopotential, as is discussed by Heine and Lee.[7] Thus, although his pseudopotential is correctly screened in the long- and short-wavelength limits, it might not be accurate for the intermediate region of wavelength. We believe that the screening effects in copper can be represented approximately by Lindhard's dielectric function δ. For the heavier transition metals, however, we would certainly have to modify our dielectric function, because a translationally invariant form of dielectric function is no longer even approximately valid due to the predominance of d electrons at the Fermi surface This modification can be incorporated in the present method in a straightforward manner.

TABLE VIII. Comparison of the results for the point-mass enhancement factor λ_k and the relaxation time τ_k for copper with those given in the literature.

	Lee[a]	Teichler[b]	Nowak[c]	Koch and Doezema[d]	Present work
λ_{100}	0.211 ± 0.014	0.086	0.21	•••	0.175 ± 0.017
λ_{110}	0.038 ± 0.012	0.164	0.10	•••	0.086 ± 0.009
λ_{111}	0.219 ± 0.012	0.185	0.17	•••	0.232 ± 0.023
λ_{av}	•••	0.151	0.12 ± 0.02	•••	0.150 ± 0.02
$\frac{1}{\tau_{100}}$ (10^7 sec^{-1}/°K^3)	•••	•••	0.580	1.15 ± 0.05	1.2
$\frac{1}{\tau_{110}}$ (10^7 sec^{-1}/°K^3)	•••	•••	0.115	0.12 ± 0.05	0.12
$\frac{1}{\tau_{111}}$ (10^7 sec^{-1}/°K^3)	•••	•••	4.8	3.5 ± 0.18	5.5

[a]See Ref. 5. [b]See Ref. 9. [c]See Ref. 10. [d]See Ref. 12.

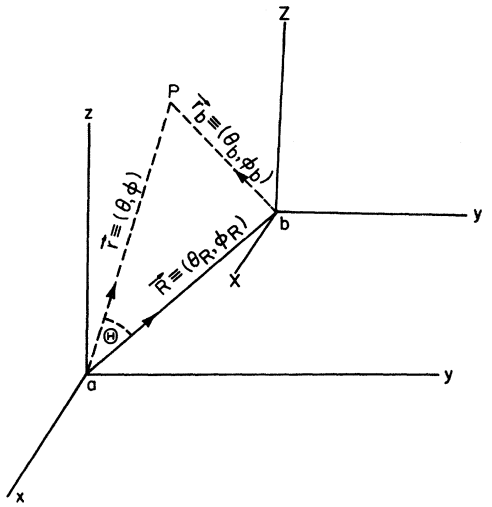

FIG. 5. Coordinate system of two nearest-neighbor atoms a and b.

Nowak's method has an advantage for nontransition metals in that screening effects are taken into account empirically. However, owing to the more complicated screening effects involved, it is unclear whether the method can be extended to calculate electron-phonon–interaction effects in the heavier transition metals.

An important advantage of the present approach in calculating the matrix elements of the electron-phonon interaction is that matrix elements between states of different energies can be calculated. These matrix elements, which cannot be derived from Golibersuch's formalism, are essential to calculate the phonon dispersion relations, as has been mentioned by Sinha.[3]

The discrepancy between the present results for $\lambda_{\vec{k}}$ and those obtained by Teichler,[9] who obtained a reasonably good average value of λ using the Wannier-function representation and a rather crude model for the phonon spectrum, clearly demonstrates the importance of the phonon-polarization effects and the umklapp processes in the anisotropy of the electron-phonon interaction. The average value $\lambda_{av} = 0.15 \pm 0.02$ of the velocity-renormalization constant derived from the relation

$$\lambda_{av} = \tfrac{1}{26}(6\lambda_{100} + 12\lambda_{110} + 8\lambda_{111}) \qquad (22)$$

is consistent with the value $\lambda_{av} = 0.10 \pm 0.01$ inferred by Nowak and Lee[28] from experimental data.

Thus essentially we have developed a rapidly convergent and comparatively inexpensive method of calculating the electron-phonon–interaction matrix elements based on the OPW tight-binding method, and it can be used to investigate such effects in transition metals. Also, it is essential to consider explicitly the effect of phonon polarization and umklapp processes in order to understand the anisotropic nature of the electron-phonon interaction. The existence of such anisotropies in superconductors should be tested experimentally. The possibility of such experiments is now enhanced with the recent techniques of phonon generation by Narayanmurti.[29]

From the good agreement of the present results and those of Nowak with Lee's interpretation of the experimental data, it is fair to conclude that a proper understanding of the electron-phonon interaction in copper has now been achieved. One of the immediate applications of the present method will be to investigate the superconducting transition metals. It would be highly interesting to apply the present formulation to make a similar investigation of the fifth-band sheet of the Fermi surface of palladium. This band is known to have a large cyclotron mass, and the Fermi energy occurs on the single-particle density-of-states curve in a region where the latter has large first and second derivatives.[30] One therefore anticipates a large effect of the electron-phonon interaction on the Fermi-surface properties[17] on this sheet. This speculation is based on similar changes observed in the fifth-band sheet of the palladium Fermi surface as a result of large hydrostatic pressure,[17] and also from positron-annihilation studies as a function of pressure in palladium.[31] Another immediate application is to calculate the phonon-dispersion relation using this model. We hope to return to this problem in the near future.

ACKNOWLEDGMENTS

I am highly indebted to Dr. M. H. Cohen and Dr. Martin J. G. Lee for their helpful guidance in the last stages of this work. My thanks are due to Dr. F. M. Mueller for suggesting the problem and for his continued interest in the work, to Dr. G. Das, Dr. S. K. Sinha, and Dr. J. Robinson for many helpful discussions and suggestions, to Dr. O. C. Simpson for sponsoring this work, to Dr. David Price for making available his computer program for obtaining the phonon spectrum, to the Chemistry Division of Argonne National Laboratory for letting me use their computer facilities, to the ANL computation center for their excellent service and cooperation, and to the secretaries of the Solid State Science Division for their excellent typing service.

APPENDIX A

Here will be derived the electron-phonon matrix elements between the tight-binding d states $\varphi^{\vec{k}}_{dm}$ and $\varphi^{\vec{k}'}_{dm'}$, which run as

$$\langle \varphi^{\vec{k}}_{\vec{d}m} | g_{\vec{q}\lambda}(\vec{r}) | \varphi^{\vec{k}'}_{\vec{d}m'} \rangle \approx \sum_{R_l} e^{-i\vec{k}\cdot\vec{R}_l} \int \varphi^*_{\vec{d}m}(\vec{r}-\vec{R}_l) g_{\vec{q}\lambda}(\vec{r}) \varphi_{\vec{d}m'}(\vec{r})\, d^3r + \sum_{R_l} e^{i\vec{k}\cdot\vec{R}_l} \int \varphi^*_{\vec{d}m}(\vec{r}) g_{\vec{q}\lambda}(\vec{r}) \varphi_{\vec{d}m'}(\vec{r}-\vec{R}_l)\, d^3r$$
$$+ \sum_{R_l} e^{i(\vec{k}'-\vec{k})\cdot\vec{R}_l} e_{q\lambda} \int \varphi^*_{\vec{d}m}(\vec{r}-\vec{R}_l) \varphi_{\vec{d}m'}(\vec{r}-\vec{R}_l) g_{\vec{q}\lambda}(\vec{r})\, d^3r \quad , \tag{A1}$$

$\vec{R}_l$ going over the nearest neighbors. First the integral

$$I_{q,mm'} = \int \varphi^*_{\vec{d}m}(\vec{r}) g_{\vec{q}\lambda}(\vec{r}) \varphi_{\vec{d}m'}(\vec{r}-\vec{R}_l)\, d^3r = \left(\frac{\hbar}{2M\omega_{\vec{q}\lambda}\Omega_0}\right)^{1/2} \int \varphi^*_{\vec{d}m}(\vec{r}) \nabla V(r)\, e_{\vec{q}\lambda} \varphi_{\vec{d}m'}(\vec{r}-\vec{R}_l)\, d^3r \tag{A2}$$

will be considered. As the potential is spherically symmetric, $\nabla V(r) = (dV/dr)\hat{r}$. The screened potential is given by

$$V(r) = \int \epsilon^{-1}(r, r') V_c(r')\, d^3r' = \frac{1}{(2\pi)^3} \iint \frac{1}{\epsilon(q,0)} e^{-i\vec{q}\cdot(\vec{r}-\vec{r}')} V_c(r')\, d^3r'\, d^3q = \frac{1}{(2\pi)^3} \int \frac{V_c(q')}{\epsilon(q,0)} e^{-i\vec{q}\cdot\vec{r}}\, d^3q \quad .$$

Thus,

$$\hat{r}\cdot\nabla V(r) = \frac{dV}{dr} = \frac{-1}{(2\pi)^3} \int e^{-i\vec{q}\cdot\vec{r}} \frac{V_c(q)}{\epsilon(q,0)} i\vec{q}\cdot\hat{r}\, d^3q$$
$$= \frac{-1}{(2\pi)^3} \int \sum_{l=0}^{\infty} i^l 4\pi(2l+1) j_l(qr) Y^0_L(\theta_q) \frac{V_c(q)}{\epsilon(q,0)} q^3 \cos\theta_q \sin\theta_q\, d\theta_q\, d\varphi_q\, dq$$
$$= \frac{4\pi}{(2\pi)^3} \int_0^{\infty} q^3 j_1(qr) \frac{V_c(q)}{\epsilon(q,0)}\, dq = \frac{1}{2\pi^2}\, w(r) \quad , \tag{A3}$$

where

$$w(r) = \int_0^{\infty} q^3 j_1(qr) [V_c(q)/\epsilon(q,0)]\, dq \quad . \tag{A4}$$

Now

$$\varphi_{\vec{d}m}(\vec{r}-\vec{R}) = \sum_p C_p A_p r_b^2 e^{-t_p|\vec{r}-\vec{R}|} Y_{2m'}(\theta_b, \varphi_b) = \sum_{t\mu} B_{m't\mu}(\hat{R}) r^t R^{2-t} Y_{t\mu}(\theta,\varphi) \sum_p A_p C_p e^{-t_p|\vec{r}-\vec{R}|}, \quad 2 \geq t \geq |\mu| \tag{A5}$$

where the constants $B_{mt\mu}(\hat{R})$ depend on the coordinate systems chosen and the definition of the functions $Y_{lm'}$, i.e., whether they are defined to be complex or real functions. The derivation of the expression for $B_{mt\mu}(\hat{R})$ is given in Appendix B.

Expanding $e^{-t|\vec{r}-\vec{R}|}$ in terms of Bessel functions of imaginary arguments and half-integral orders,

$$\frac{e^{-t|\vec{r}-\vec{R}|}}{|\vec{r}-\vec{R}|} = \xi \sum_{l=0}^{\infty} (2l+1) i_l(\xi r_<) k_l(\xi r_>) P_l(\cos\Theta) \quad , \quad r_{\substack{<\\>}} \equiv (r, R)^{\min}_{\max}$$

whence

$$e^{-t|\vec{r}-\vec{R}|} = -\sum_{l=0}^{\infty} (2l+1) i_l(\xi r_<) P_l(\cos\Theta) k_l(\xi r_>) - \xi \sum_{l=0}^{\infty} (2l+1) [r_< i_l'(\xi r_<) k_l(\xi r_>) + i_l(\xi r_<) k_l'(\xi r_>) r_>] P_l(\cos\Theta)$$
$$= \sum_{l=0}^{\infty} f_l(\xi r_<, \xi r_>) P_l(\cos\Theta) \quad , \tag{A6}$$

where

$$f_l(\xi r_<, \xi r_>) = -(2l+1)[\xi r_< i_l'(\xi r_<) k_l(\xi r_>) + \xi r_> i_l(\xi r_<) k_l'(\xi r_>) + i_l(\xi r_<) k_l(\xi r_>)] \quad . \tag{A7}$$

Substituting the expansion of dV/dr and $\varphi_{\vec{d}m}(r-R)$ in Eq. (A2),

$$I_{\vec{q},mm'} = \left(\frac{\hbar}{2M\omega_{\vec{q}\lambda}\Omega_0}\right)^{1/2} \frac{1}{2\pi^2} \sum_{\substack{lt\mu \\ l=0,1,\ldots 5 \\ 2\geq t\geq|\mu|}} B_{m't\mu}(\hat{R}) S_{lt}(|R|) \int P_l(\cos\Theta) Y_{t\mu}(\hat{r}) (\hat{r}\cdot\vec{e}_{\vec{q}\lambda}) Y^*_{2m}(\hat{r})\, d\Omega \quad , \tag{A8}$$

where

$$S_{lt}(|R|) = \sum_{pq} A_p A_q C_p C_q \int_0^{\infty} W(r) f_l(\xi_p r_<, \xi_p r_>) e^{-t_q r} r^{4+t} R^{2-t}\, dr \quad . \tag{A9}$$

The factors $S_{lt}(|R|)$ are shown in Table VI.

The integrals over the angular variable θ, φ in Eq. (A8) are given by

$$\int P_l(\cos\Theta)Y_{t\mu}(\hat{r})(\hat{r}\cdot\vec{e}_{\vec{q}\lambda})Y^*_{2m}(\hat{r})\,d\Omega$$

$$=\left(\frac{4\pi}{2l+1}\right)\sum_{m''=-l}^{l}\int Y_{lm''}(\hat{r})Y^*_{lm''}(\hat{R})\sum_{M=-1,0,1}D^M_{\vec{q}\lambda}Y_{1M}(\hat{r})(\tfrac{4}{3}\pi)^{1/2}Y^*_{2m}(\hat{r})Y_{t\mu}(\hat{r})\,d\Omega$$

$$=\frac{4\pi}{2l+1}\sum_{\substack{m''=-l\\M=-1,0,1}}^{l}Y^*_{lm''}(\hat{R})D^M_{\vec{q}\lambda}\sum_L C(t,1,L;\mu,M)C(t,1,L;0,0)\left(\frac{2t+1}{2L+1}\right)^{1/2}\int Y_{lm''}(\hat{r})Y^*_{2m}(\hat{r})Y_{L\mu+M}(\hat{r})\,d\Omega$$

$$=\left(\frac{4\pi}{2l+1}\right)^{1/2}\sum_{M=-1,0,1}\left(\frac{2t+1}{5}\right)^{1/2}Y^*_{lm-\mu-M}(\hat{R})D^M_{\vec{q}\lambda}C(t,1,L;\mu,M)C(t,1,L;0,0)C(l,L,2;m-\mu-M,\mu+M)$$

$$\times C(l,L,2;0,0),\quad L=\begin{cases}1,3,\ldots,-t+1 & \text{if } t \text{ is even}\\ 0,2 & \text{if } t=1\end{cases}\quad . \tag{A10}$$

Thus substituting in Eq. (A8) the results from Eq. (A10),

$$I_{\vec{q},mm'}=\left(\frac{\hbar}{2M\omega_{\vec{q}\lambda}\Omega_0}\right)^{1/2}\frac{1}{2\pi^2}\sum_{ltM}B_{m't\mu}(\hat{R})Y^*_{lm-\mu-M}(\hat{R})S_{lt}(|R|)D^M_{\vec{q}\lambda}\left(\frac{4\pi(2t+1)}{5(2l+1)}\right)^{1/2}\sum_L C(t,1,L;\mu,M)C(t,1,L;0,0)$$

$$\times C(l,L,2;m-\mu-M,\mu+M)C(l,L,2;0,0),$$

$$l=0,1,\ldots,5,\quad 2\geq t\geq|\mu|,\quad M=-1,0,1,\quad L=\begin{cases}0,2 & \text{if } t=1\\ 1,3,\ldots,t+1 & \text{if } t \text{ is even}\end{cases}\quad . \tag{A11}$$

Now consider the terms in which charge density is on one center and ∇V on the other:

$$\sum_{\substack{R\\\text{nearest}\\\text{neighbors}}}e^{i(\vec{k}'-\vec{k})\cdot\vec{R}}\,\vec{e}_{\vec{q}\lambda}\cdot\int\varphi^*_{dm}(\vec{r}-\vec{R})\varphi_{dm'}(\vec{r}-\vec{R})\nabla V(r)\,d^3r$$

$$=\frac{1}{(2\pi)^3}\sum_R e^{i(\vec{k}'-\vec{k})\cdot\vec{R}}\int d^3r\,\varphi^*_{dm}(\vec{r}-\vec{R})\varphi_{dm'}(\vec{r}-\vec{R})\int d^3r'\,d^3q'\,i\,\frac{1}{\epsilon(q',0)}\,e^{-i\vec{q}'\cdot(\vec{r}-\vec{r}')}V_c(r')\vec{q}'\cdot\vec{e}_{\vec{q}\lambda}$$

$$=\frac{1}{(2\pi)^3}\sum_R e^{i(\vec{k}'-\vec{k})\cdot\vec{R}}\int\frac{d^3q'e^{-i\vec{q}'\cdot\vec{R}}}{\epsilon(q',0)}\,i\vec{q}'\cdot\vec{e}_{\vec{q}\lambda}V_c(q')\int d^3r\,\varphi^*_{dm}(\vec{r}-\vec{R})\varphi_{dm'}(\vec{r}-\vec{R})\,e^{-i\vec{q}'\cdot(\vec{r}-\vec{R})}$$

$$=\frac{4\pi}{(2\pi)^3}\sum_R e^{i(\vec{k}'-\vec{k})\cdot\vec{R}}\int d^3q'\,e^{-i\vec{q}'\cdot\vec{R}}\,i\vec{q}'\cdot\vec{e}_{\vec{q}\lambda}\,\frac{V_c(q')}{\epsilon(q',0)}$$

$$\times\sum_{L=0,2,4}(i)^L f_L(q')Y_{Lm'-m}(\hat{q}')C(2,L,2;m,m'-m)C(2,L,2;0,0)\quad ,$$

where

$$f_L(q')=\left(\frac{2L+1}{4\pi}\right)^{1/2}\sum_{lt}C_sC_tA_sA_t\int r^6j_L(q'r)\,e^{-i(\xi_t+\xi_s)r}\,dr \tag{A12}$$

and the C's are th Clebsch–Gordan coefficients. Expanding the term $-e^{-i\vec{q}'\cdot\vec{R}}$ in terms of Bessel functions, noting that the q' vector gives spherical harmonics of angular momentum one, and substituting Eq. (A12) into (A1), one gets Eq. (19).

APPENDIX B

$B_{mt\mu}$ enters the expression for $\varphi_{2m}(\vec{r}-\vec{R})\equiv\varphi_{2m}(r_b)$ through the relation

$$r_b^2Y_{2m}(\theta,\varphi_b)=\sum_{\substack{t\mu\\2>t>\mu}}B_{mt\mu}(\hat{R})r^tR^{2-t}Y_{t\mu}(\theta,\varphi)\quad . \tag{B1}$$

Let the atom b be situated at the point $\vec{R}\equiv(X,Y,Z)$ in the coordinate system centered at a(see Fig. 5)

$$\vec{r}_b=\vec{r}-\vec{R}\quad .$$

First consider the case $m=0$:

$$r_b^2Y_{20}(\theta_b,\varphi_b)=N_{20}(r_b^2/2)(3\cos^2\theta_b-1)=N_{20}\tfrac{1}{2}(3z_b^2-r_b^2)=N_{20}\tfrac{1}{2}[3(z-Z)^2-(r-R)^2]$$

$$=N_{20}\quad[(3z^2-r^2)+(3Z^2-R^2)-6rR\cos\theta\cos\theta_R+2rR\cos\Theta]$$

$$= r^2 Y_{20}(\theta, \varphi) + R^2 Y_{20}(\theta_R, \varphi_R) - N_{20}(3rR\cos\theta\cos\theta_R - rR\cos\Theta),$$

where $N_{20} = (5/4\pi)^{1/2}$.

Substituting for $\cos\Theta = \cos\theta\cos\theta_R + \sin\theta\sin\theta_R\cos(\varphi - \varphi_R)$, one gets

$$r_b^2 Y_{20}(\theta_b, \varphi_b) = r^2 Y_{20}(\theta, \varphi) + R^2 Y_{20}(\theta_R, \varphi_R) - rRN_{20}[3\cos\theta\cos\theta_R - \cos\theta\cos\theta_R - \tfrac{1}{2}\sin\theta\sin\theta_R(e^{i(\varphi-\varphi_R)} + e^{-i(\varphi-\varphi_R)})]$$
$$= r^2 Y_{20}(\theta, \varphi) + R^2 Y_{20}(\theta_R, \varphi_R) - rRN_{20}\{2Y_{10}(\theta_R, \varphi_R)Y_{10}(\theta, \varphi)/N_{10}^2$$
$$- (1/2N_{11}^2)[Y_{11}(\theta, \varphi)Y_{11}^*(\theta_R, \varphi_R) + Y_{1-1}(\theta, \varphi)Y_{1-1}^*(\theta_R, \varphi_R)]\}\ , \quad \text{(B2)}$$

where

$$N_{00} = 1/(4\pi)^{1/2}, \quad N_{10} = 3/(4\pi)^{1/2}, \quad N_{11} = -3/(8\pi)^{1/2}\ . \quad \text{(B3)}$$

Thus, by comparison with Eq. (B1) one gets the values of $B_{0t\mu}(R)$ listed in Table III.

Next consider the case $m = 2$:

$$r_b^2[Y_{22}(\theta_b, \varphi_b) + Y_{22}(\theta_b, \varphi_b)] = N_{22}(X_b^2 - Y_b^2) = N_{22}[(x - X)^2 - (y - Y)^2] = N_{22}[(x^2 - y^2) + (X^2 - Y^2) - (xX - yY)]$$
$$= r^2[Y_{22}(\theta, \varphi) + Y_{2-2}(\theta, \varphi)] + R^2[Y_{22}(\theta_R, \varphi_R) + Y_{2-2}(\theta_R, \varphi_R)] - N_{22}(xX - yY)\ .$$

But

$$xX - yY = \tfrac{1}{2}[(x + iy)(X + iY) + (X - iY)(x - iy)] = \tfrac{1}{2}rR\sum_{m=1,-1}[y_{1m}(\theta, \varphi)Y_{1m}(\theta_R, \varphi_R)]\ .$$

Thus,

$$r_b^2[Y_{22}(\theta_b, \varphi_b) + Y_{2-2}(\theta_b, \varphi_b)] = r^2[Y_{22}(\theta, \varphi) + Y_{2-2}(\theta, \varphi)] + R^2[Y_{22}(\theta_R, \varphi_R) + Y_{2-2}(\theta_R, \varphi_R)]$$
$$- (N_{22}/2N_{11}^2)rR[Y_{11}(\theta, \varphi)Y_{11}(\theta_R, \varphi_R) + Y_{1-1}(\theta, \varphi)Y_{1-1}(\theta_R, \varphi_R)]\ . \quad \text{(B4)}$$

Here

$$N_{22} = (15/8\pi)^{1/2}. \quad \text{(B5)}$$

Similarly,

$$r_b^2[Y_{22}(\theta_b, \varphi_b) - Y_{2-2}(\theta_b, \varphi_b)] = N_{22}2i(x_b y_b) = N_{22}2i(x - X)(y - Y)$$
$$= r^2[Y_{22}(\theta, \varphi) - Y_{2-2}(\theta_R, \varphi_R)] + R^2[Y_{22}(\theta_R, \varphi_R) - Y_{2-2}(\theta_R, \varphi_R)] - N_{22}2i(xY + yX)$$
$$= r^2[Y_{22}(\theta, \varphi) - Y_{2-2}(\theta_R, \varphi_R)] + R^2[Y_{22}(\theta_R, \varphi_R) - Y_{2-2}(\theta_R, \varphi_R)]$$
$$- rR(N_{22}/N_{11}^2)[Y_{11}(\theta, \varphi)Y_{11}(\theta_R, \varphi_R) - Y_{1-1}(\theta, \varphi)Y_{1-1}(\theta_R, \varphi_R)]\ . \quad \text{(B6)}$$

Adding Eqs. (B4) and (B6), one gets

$$r_b^2 Y_{22}(\theta_b, \varphi_b) = rR\,Y_{22}(\theta, \varphi) + R^2 Y_{22}(\theta_R, \varphi_R) - rR\ (N_{22}/N_{11}^2)Y_{11}(\theta, \varphi)Y_{11}(\theta_R, \varphi_R)\ , \quad \text{(B7)}$$

and similarly

$$r_b^2 Y_{2-2}(\theta_b, \varphi_b) = r^2 Y_{2-2}(\theta, \varphi) + R^2 Y_{2-2}(\theta_R, \varphi_R) - rR\ (N_{22}/N_{11}^2)Y_{1-1}(\theta, \varphi)Y_{1-1}(\theta_R, \varphi_R)\ . \quad \text{(B8)}$$

Comparing Eqs. (B7) and (B8) with Eq. (B1), one gets the expression for $B_{2t\mu}(\hat{R})$ and $B_{-2t\mu}(\hat{R})$ listed in Table III. One can proceed identically and get the rest of the constant $B_{mt\mu}(\hat{R})$ listed in Table III.

---

*Based on work performed under the auspices of the U. S. Atomic Energy Commission. The paper is submitted for partial fulfillment of the thesis requirements for the Ph.D. degree at the University of Chicago.

[1]W. L. McMillan, Phys. Rev. **167**, 331 (1968).

[2]Philip B. Allen and Marvin L. Cohen, Phys. Rev. **187**, 525 (1969), and references therein.

[3]S. K. Sinha, Phys. Rev. **169**, 477 (1968).

[4]D. C. Golibersuch, Phys. Rev. **157**, 532 (1967).

[5]Martin J. G. Lee, Phys. Rev. B **2**, 250 (1970).

[6]P. B. Allen and M. J. G. Lee (unpublished).

[7]Volker Heine and Martin J. G. Lee, Phys. Rev. Lett. **27**, 811 (1971).

[8]S. T. Chui (unpublished).

[9]H. Teichler, Phys. Status Solidi B **48**, 189 (1971).

[10]David Nowak, Phys. Rev. B **6**, 3691 (1972).

[11]V. F. Gantmakher, Phys. Rev. B (to be published).

[12]J. F. Koch and R. E. Doezema, Phys. Rev. Lett. **24**, 507 (1970); R. E. Doezema and J. F. Koch, Phys. Rev. B **6**, 207 (1972).

[13]N. E. Christansen, Solid State Commun. **9**, 479 (1971).

[14]L. Hedin and S. Lundquist, in *Solid State Physics*, edited by F. Seitz, D. Turnbull, and H. Ehrenreich (Academic, New York, 1970), Vol. 23.

[15]F. M. Mueller, Phys. Rev. **153**, 659 (1967).

[16]L. J. Sham, Proc. R. Soc. Lond. **78**, 895 (1961).

[17]S. G. Das, D. D. Koelling, and P. M. Mueller, Solid State Commun. **12**, 89 (1973).

[18]N. O. Lipari and R. A. Deegan, Solid State Commun. **9**, 1481 (1971).
[19]G. A. Burdick, Phys. Rev. **129**, 138 (1963).
[20]A. C. Wahl *et al.*, ANL Report No. 7271 (unpublished).
[21]The error we have committed in choosing the *d* states as valid for atomic copper is of the order of 20%. Also the *d* character of the band state varies from 10 to 40% on the Fermi surface and the contribution from *s-d* hybridization to the matrix elements is of the order of 3.3% of that from the plane waves. Hence the error in the matrix elements is $\lesssim 5\%$.
[22]J. M. Ziman, in *The Physics of Metals*, edited by J. M. Ziman, (Cambridge U. P., Cambridge, England, 1969), p. 256.
[23]M. J. G. Lee, Phys. Rev. **187**, 901 (1969).
[24]F. M. Mueller *et al.*, ANL Report No. 7556 (unpublished).
[25]E. C. Srensson, B. N. Brockhouse, and J. M. Rowe, Phys. Rev. **155**, 619 (1967).
[26]S. K. Sinha and R. P. Gupta (unpublished).
[27]S. Barisic, Phys. Rev. B **5**, 932 (1972).
[28]D. Nowak and Martin J. G. Lee, Phys. Rev. B **5**, 2851 (1972).
[29]V. Narayanmurti, Bull. Am. Phys. Soc. **17**, 117 (1972).
[30]S. G. Das and F. M. Mueller (unpublished).
[31]A. S. Klotz (private communication).
[32]F. M. Mueller, A. J. Freeman, J. O. Dimmock, and A. Furdyna, Phys. Rev. B **1**, 4617 (1970).

PHYSICAL REVIEW B VOLUME 7, NUMBER 6 15 MARCH 1973

Electrical Conductivity in Disordered Systems

J. Bernasconi
Brown Boveri Research Center, CH-5401 Baden, Switzerland
(Received 11 September 1972)

We investigate the temperature dependence of the hopping conductivity in a system in which hopping only takes place between nearest-neighbor centers. The system is simulated by a disordered classical-resistance network and analyzed in terms of percolation along critical paths and in terms of an effective-medium theory. The model is applied to the recent small-metal-particle experiments of Zeller.

I. INTRODUCTION

In recent years transport phenomena in disordered systems have aroused great interest among experimental and theoretical physicists.[1-8] The thermally activated hopping of charged particles (electrons, ions) between localized centers is considered one of the most important mechanisms for the description of electrical conduction in such disordered or amorphous materials. The transition rate p for the hopping (tunneling) between two well-localized centers is generally assumed to be of the form[2,3]

$$p = p_0 e^{-2\alpha r} e^{-\beta \Delta E}, \quad \beta = 1/k_B T . \tag{1}$$

p_0 is a constant depending on the properties of the material, but not on r, T, or ΔE, r is the distance between the centers, ΔE is the activation energy for the hopping process, and α^{-1} is the decay length of the (electron, ion) wave function localized at a single center.

Mott[2] has argued that in a disordered system ΔE should be of the form

$$\Delta E \propto 1/N(E_F) r^3 , \tag{2}$$

where $N(E_F)$ is the density of states at the Fermi level. By maximizing p with respect to r, Mott then predicted the temperature dependence of the dc electrical conductivity σ to be described by the law

$$\ln(\sigma/\sigma_0) \propto -\beta^{1/4} . \tag{3}$$

Equation (3) should be valid for not too high temperatures and is indeed found to be consistent with, e.g., the dc conductivity data of amorphous germanium in the temperature range $50 \lesssim T \lesssim 300$ K (see Refs. 2 and 3 and the references cited therein).

Starting from Mott's model, Ambegaokar *et al.*[3] have assumed that the centers are randomly distributed in space and that the energies of the electronic states, localized at the centers, are also random in a region around the Fermi energy. Then they are able to formulate the problem in terms of a classical-resistance network and derive Mott's law (3) from percolation considerations.

Kirkpatrick[7] investigates some general properties of disordered classical-resistance networks. He especially discusses the results of a critical-path analysis and those of an effective-medium theory by comparing them with numerically calculated conductivities of some random networks (i.e., networks in which the values of the individual conductances are distributed according to some probability law).

In this paper the temperature dependence of the hopping conductivity in a system in which hopping only takes place between nearest-neighbor centers is investigated and discussed. This means that we assume the transition rate p_{ij} for the hopping between centers i and j to have the form

$$p_{ij} = p_0 e^{-\beta E_{ij}} \quad \text{if } i,j \text{ are nearest neighbors}$$
$$= 0 \quad \text{otherwise.} \tag{4}$$